The 2009 IEEE/RSJ International Conference on
Intelligent Robots and Systems
October 11-15, 2009 St. Louis, USA

Experimental Evaluation of Optimal Conically-Shaped Dielectric Elastomer Linear Actuators

Giovanni Berselli, Rocco Vertechy, Gabriele Vassura and Vincenzo Parenti Castelli

***Abstract*— A conically shaped Dielectric Elastomer (DE) linear actuator is presented which is obtained by coupling a DE film with a compliant mechanism. The compliant mechanism is designed, by means of a pseudo-rigid-body model, to suitably modify the force generated by the elastomer film. The resulting actuator provides a nearly constant force along the entire actuator stroke when the DE film is activated and returns to an initial rest position when the DE film is deactivated. Experimental activity fully validates the proposed concept. Possible applications of this kind of actuator are Braille cells, light weight robots and haptic devices.**

***Index Terms*— Dielectric Elastomer actuators, compliant mechanisms.**

I. Introduction

Among the class of materials known as electroactive polymers, Dielectric Elastomers (DEs) represent one of the best materials that can be used for the development of linear actuators. DE based actuators offer high power density and good efficiencies combined with relatively low weight and extremely low costs.

In practice a DE is a deformable dielectric which can experience deviatoric (isochoric) finite deformations in response to applied large electric fields while, at the same time, alter the applied electric fields in response to the deformations undergone [1], [2]. For actuation usage, DEs are usually shaped in thin sheets coated with compliant electrodes on both sides and piled one on the other to form a multilayer DE [3]. Activation of the DE via the placement of differential electric potentials (hereafter also called voltages) between the electrodes can induce film area expansions and, thus, point's displacements which can be used to produce useful mechanical work (whenever forces are applied to such points).

Different kinds of DE actuators with various shapes have been proposed in the literature [4], [5], [2]. In particular, previous work done by Vogan [6] and Berselli et al. [7] has shown that the overall behavior of a DE actuator can be improved by coupling the DE film with a compliant mechanism (hereafter also referred to as frame). This frame can be specifically designed to modify the overall actuator stiffness which heavily depends on the DE's elastic properties. For instance, depending on the frame design, the actuator can work monodirectionally [8] or bidirectionally as long as the frame's own stiffness can be used to provide a restoring force

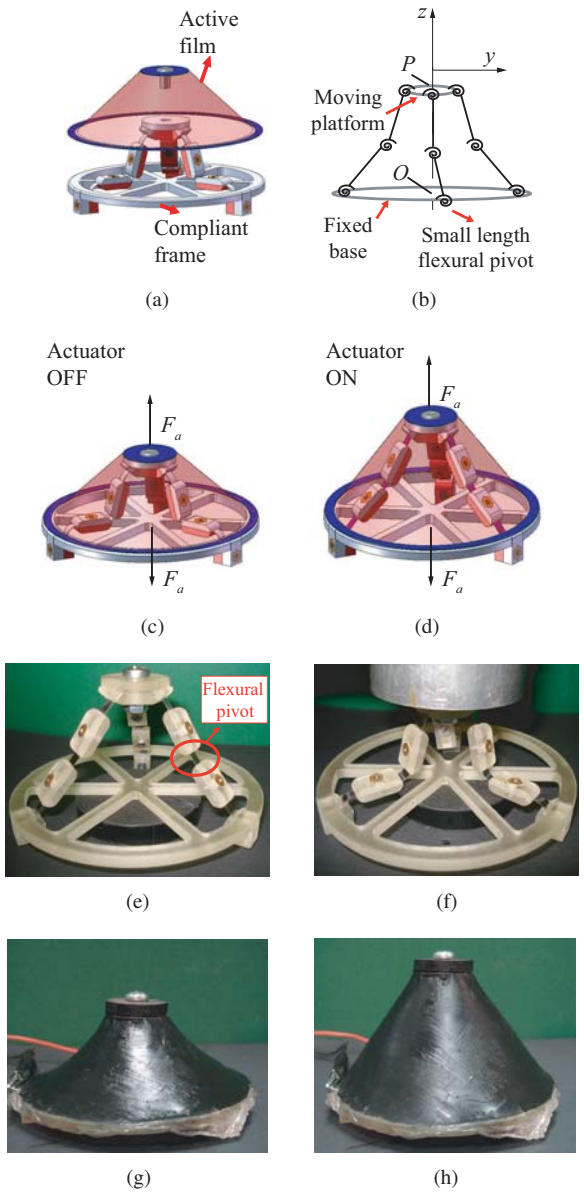

Fig. 1. Concept behind the proposed solution and actuator prototype. Assembly exploded view (a), compliant frame schematic (b), CAD model in deactivated (c) and activated (d) states, frame prototype in undeflected condition (e) and under constant load application (f), actuator in deactivated (g) and activated (h) states.

Giovanni Berselli is a Ph.D. student at DIEM, Mechanical Eng. Dept., University of Bologna, Viale Risorgimento 2, 40136 Bologna, Italy (phone: +393358092364; fax: +39059731515; email: giovanni.berselli@unibo.it.)

Rocco Vertechy is Assistant Professor at PERCRO, Scuola Superiore Sant'Anna, Via Rinaldo Piaggio, 34, 56025 Pontedera (PI), Italy (email: r.vertechy@sssup.it.)

Gabriele Vassura is Associate Professor at DIEM (email: gabriele.vassura@unibo.it.)

Vincenzo Parenti Castelli is Full Professor at DIEM (email: vincenzo.parenti@unibo.it.)

that brings back the actuator to an initial position when the DE is deactivated. Furthermore, particular frame designs can be used so as to obtain a constant available thrust over a given range of motion.

The objective of the present paper is to design a DE linear actuator capable of supplying a constant force over a given range of motion when activated, and of returning to an initial rest position when deactivated by showing a behavior similar to a one dimensional linear spring. Design solutions for obtaining constant force DE actuators have been proposed in [6], [7] concerning DE films which are shaped as lozenges and in [8] concerning DE films which are shaped as rectangles. The authors themselves remarked both the advantages and the critical aspects of such designs.

This paper investigates a different solution when compared to previously published works. The proposed design employs a DE film of conical shape similar to the one proposed by Plante et al. [9]. However, the actuator proposed in [9] supplies an available thrust that heavily changes along the stroke. This behavior is hereafter modified by coupling the conical DE film with a compliant frame designed as an overconstrained parallel mechanism having three equal legs articulated via three revolute joints with parallel axes. The CAD exploded view of the actuator is shown in Fig. 1(a), the schematic of the compliant frame is shown in Fig. 1(b) whereas the actuator CAD models showing the coupling between the DE film and the frame are shown in Figs. 1(c),1(d). With reference to Fig. 1(b), displacements of the moving platform along the radial, y, direction (or, alternatively, rotations) are prevented by the parallel tripod architecture. The revolute joints of the parallel mechanism are designed as "Small-length Flexural Pivots" [10], [11] i.e. as short flexible segments whose resistance to deflection is modeled using a torsional spring.

In this paper, the electromechanical properties of the DE film are measured experimentally. A pseudo-rigid model of the compliant frame is derived and used for the initial sizing of the small-length flexural pivots. Experimental activity is then used to verify the behavior of the frame and of the overall actuator prototype. In particular, the frame prototype is shown in Fig. 1(e) (undeflected condition) and in Fig. 1(f) (moving platform loaded with a constant load acting in the z direction). The overall actuator prototype is depicted in Fig. 1(g) (actuator deactivated state) and in Fig. 1(h) (actuator activated state).

Possible applications of this kind of actuator are Braille cells [5], lightweight robots [4] and haptic devices [12].

II. Achievement of Constant Force Actuators

In general, the DE film deformation produces a variation of the actuator length $l = |(P - O)|$, where P and O are, for instance, two points of the actuator lying on the DE film's axis of symmetry (Fig. 1(b)), and a force having the same direction of vector $\overline{OP}$ that can be supplied to an external user. This force, called the actuator available thrust, F_a, is the resultant of two internal forces:

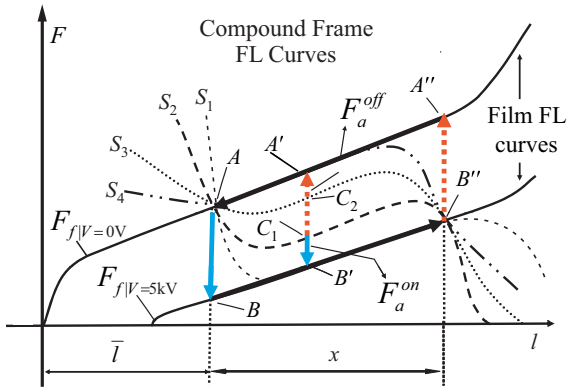

Fig. 2. FL curves qualitatively showing the moduli of F_f and F_s.

- The frame reaction force, F_s, due to the frame own stiffness, is a function of the actual actuator configuration. The flexible frame behaves, in general, like a non-linear compression spring coupled in parallel with the DE.
- The DE film force F_f which represents the resultant force in the actuation direction, defined by vector $\overline{OP}$, due to the stress field arising in the DE. This field depends on the amount of given pre-stretch, on the applied voltage, and on the actuator configuration. If material viscoelasticity and hysteresis are neglected, the film behaves, in general, as a non-linear tension spring.

The force F_a is therefore given by the difference between the film and the frame forces ($F_a = F_f - F_s$). Conventionally, F_a is the force that an external user supplies to the actuator.

Let us define $l = \bar{l} + x$ as the actual actuator length where $\bar{l}$ is the actuator initial length under no load and no voltage and x is the actual actuator stroke. Figure 2 shows qualitative diagrams of Force vs actuator Length (FL) curves concerning internal forces F_f and F_s, adopting a representation methodology widely used in the study of interacting elastic structures where the moduli of the forces are shown. For simplicity, Fig. 2 assumes that the force curve F_f of the activated DE is parallel to the force curve of the deactivated DE (this is not always the case). It can be seen that a voltage application (DE film activation) causes the force F_f to drop. An actuator working cycle [6] is represented by the path $\overline{ABB''A''}$. For given F_f curves, the frame F_s curves can be designed in order to obtain an actuator capable of providing a quasi-constant force over a given range of motion. Let us propose to couple the DE with a compliant mechanism whose elastic reaction force increases as the distance $|P - O|$ increases during the outstroke. In Fig. 2 four different FL curves for F_s are depicted by assuming that the actuator stroke x and initial length $\bar{l}$ are invariant.

Consider first, the frame FL curve S_2. It can be seen that, for a large part of the stroke, F_a maintains a constant value, $F_a{}^{on}$, equal to the distance $\overline{B'C_1}$ if the DE film is activated, whereas it maintains a constant value, $F_a{}^{off}$, equal to the

distance $\overline{A'C_1}$ if the DE film is deactivated. If the actuator is required to supply a larger thrust when the DE film is active (actuator ON-state mode), a frame FL profile similar to curve S_3 can be chosen, so as to increase $F_a{}^{on}$ from $\overline{B'C_1}$ to $\overline{B'C_2}$ (and consequently decrease $F_a{}^{off}$). The OFF-state mode actuator thrust $F_a{}^{off}$ is maximized by designing a frame that provides a FL profile similar to curve S_1 whereas the ON-state mode actuator thrust $F_a{}^{on}$ is maximized by designing a frame that provides a FL profile similar to curve S_4. In such a case, however, no restoring force can pull back the actuator to its initial position when the voltage is switched off (actuator OFF-state mode) and a returning device has to be provided. Alternatively, the frame can be designed to maintain a restoring force, $F_a{}^{off}$, to a minimum sufficient to overcome the system internal dissipative forces during actuator backstroke.

III. Proposed Solution Concept

The concept behind the proposed solution is shown in Figs. 1 and 3. Similar to the definition used in Section II, the actuator length is defined as $l = |(P - O)|$, where P and O are, for instance, two points of the actuator lying on the DE film's axis of symmetry (Fig. 3). In such a case, the available thrust F_a is applied at point P and has the same direction as the vector $\overline{OP}$.

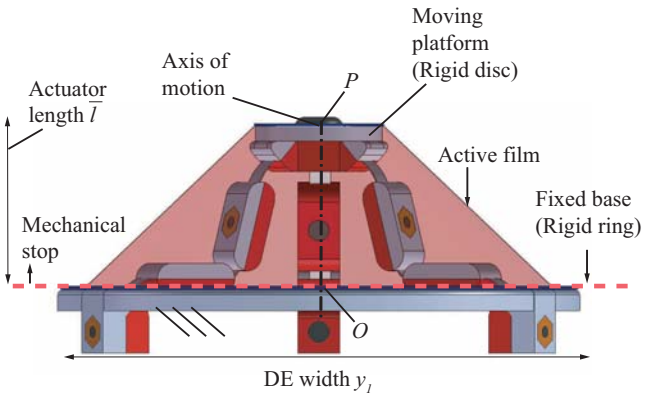

Fig. 3. Actuator configuration under no load and no voltage.

The proposed frame is designed to support the DE film (via a rigid ring and a rigid disc (Fig. 3)) and, at the same time, provide the desired FL profile. As said, the compliant frame is designed as an overconstrained parallel mechanism featuring a moving platform (the rigid disc), a fixed base (the rigid ring), and three equal legs articulated via three revolute elastic joints with parallel axes. With reference to Fig. 1(b), displacements of the moving platform along the radial, y, direction (or, alternatively, rotations) are prevented by the parallel tripod architecture. Thanks to the mechanism symmetry and to the adoption of elastic joints, each leg behave as a compliant slider-crank mechanism. A schematic model of the proposed frame is shown in Fig. 1(b). As stated before, the active film is shaped as a truncated cone. Regarding actuator manufacturing, a circular DE film with

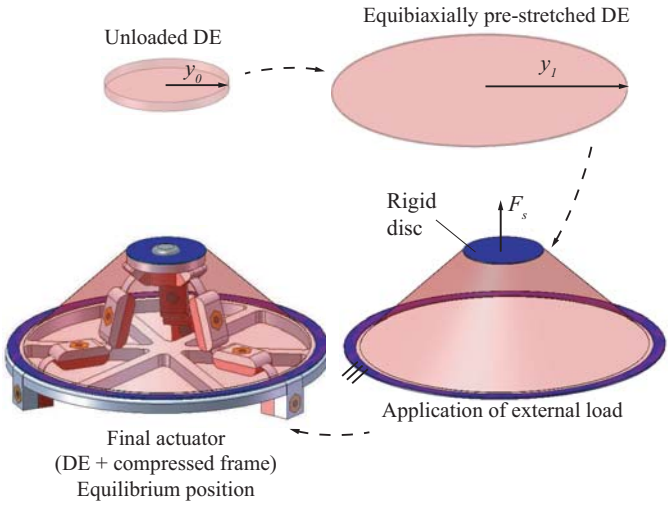

Fig. 4. Production steps for the manufacture of the actuator.

initial radius of y_0 is first subjected to an equibiaxial pre-stretch up to a final radius denoted as y_1 (Fig. 4). Then, the application of an external force in the z direction (which is supplied by the platform of the compliant frame) causes the DE film to gain a conical shape. The assembly process is shown in Fig. 4.

The actuator equilibrium position in the OFF-state mode is reached when the cranks of the compliant legs of the frame are perpendicular to the direction of motion of the moving platform. On the other hand, the fixed base provides a mechanical stop that prevents the actuator from operating in regions where $l < \bar{l}$ (Fig. 3).

The compliant frame needs to be suitably dimensioned for the specific application. The structural dimensions of the flexures can be determined, in the initial design stage, using a Pseudo-Rigid-Body Model (PRBM) of the mechanism.

IV. Model Development

The actuator available thrust is given by:

$$F_a(V, l) = F_f(V, l) - F_s(l) \tag{1}$$

where l is the actuator length and V is the voltage applied to the DE film.

A. Experimental determination of the film reaction force

The DE film used in this paper is a membrane of an acrylic elastomer (VHB4905) whereas the compliant electrodes are made with a conductive grease. The DE film dimensions and the maximum actuation voltage are reported in Table I where t denotes the initial thickness of the acrylic membrane and V_{max} is the maximum applied voltage. The initial prestretch in the y (radial) direction is $y_1/y_0 = 4$. It is worth to mention that the film force F_f depends on the amount of given pre-stretch [13].

Concerning the determination of the film force F_f at different actuation voltages, a measurement device has been used

TABLE I

DE FILM DIMENSIONS AND MAXIMUM ACTUATION VOLTAGE

y_o (mm)	y_1 (mm)	t (mm)	V_{max} (kV)
20	80	1.5	5

(a) (b)

Fig. 5. Experimental set up for the determination of DE film force F_f (a) and F_s (b)

(Fig. 5(a)). A positive displacement is imposed, along the z direction, to a rigid disc (Fig. 4) representing the moving platform of the compliant frame. The set up is configured such that the z positive direction is opposed to gravity. The deflection of the DE film due to its own weight is reasonably neglected.

Figure 6 shows the experimental film FL curves under different actuation voltages. It can be seen that, for a given imposed configuration, the modulus of the DE film reaction force F_f decreases when compared to the same force when no voltage is applied. Moreover the curves $F_a{}^{off}$ and $F_a{}^{on}$ are not parallel. The frame will be designed so as to obtain a constant force during the actuator ON state mode. During the OFF state mode, the actuator will maintain a positive stiffness; the higher this stiffness, the easier the actuator will return to its rest position (point A, in Fig. 2) when deactivated. Note that the FL curves shown in Fig. 6 are derived in quasi static loading condition and the response of the film force with respect to time is not considered here.

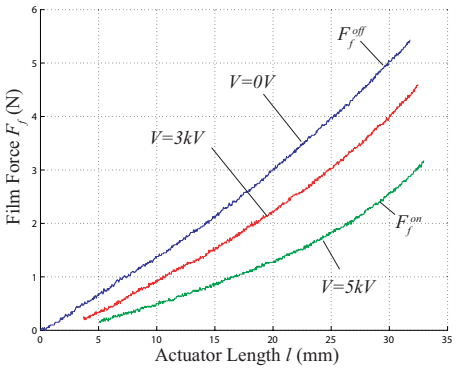

Fig. 6. DE film force under different actuation voltages, elastomer layer material = VHB4905.

B. Design of the compliant frame

A single leg of the compliant frame is modeled as a fully compliant slider-crank mechanism (Fig. 1(d)).

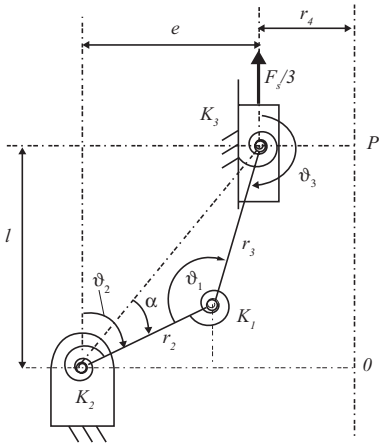

Fig. 7. Compliant frame half model schematic

The torques due to the deflection of the small length flexural pivots are given by:

$$T_i = -K_i \Psi_i \tag{2}$$

where, K_i, $i = 1, 2, 3$ are the pivot torsional stiffnesses to be designed, $\Psi_1 = \vartheta_3 - \vartheta_{30} - \vartheta_2 + \vartheta_{20}$, $\Psi_2 = \vartheta_2 - \vartheta_{20}$, $\Psi_3 = \vartheta_3 - \vartheta_{30}$, ϑ_2 and ϑ_3 are the crank and connecting rod angular positions measured with respect to the actuator's direction of motion ($\vartheta_1 = \vartheta_3 + \vartheta_2$), and ϑ_{20}, ϑ_{30}, ϑ_{10} ($\vartheta_{10} = \vartheta_{30} + \vartheta_{20}$) are the undeflected positions of the flexural pivots . Define, with reference to Fig. 7, r_2 and r_3 as the crank and the connecting-rod lengths respectively, r_4 as the distance of the slider's pivot from the actuator's axis of symmetry, and e as the slider-crank mechanism eccentricity. Recall that $l = |P - O|$ is the actual actuator length and $\bar{l}$ is the initial length of the actuator under no load an no voltage which is reached when the cranks of the compliant legs of the frame are perpendicular to the slider direction of motion. Having defined this quantities, the following relationships are found from the position analysis of the mechanism:

$$r_3 = \sqrt{\bar{l}^2 + (e - r_2)^2} \tag{3}$$

$$\vartheta_3 = \pi - asin\left(\frac{r_2 sin(\vartheta_2) - e}{r_3}\right) \tag{4}$$

$$l = r_2 cos(\vartheta_2) - r_3 cos(\vartheta_3) \tag{5}$$

Concerning the force acting on the slider, the following FL relationship can be obtained (which is verified thanks to the superimposition principle):

$$F_s = F_1 + F_2 + F_3 \tag{6}$$

where F_i concerns the contribution of the single $i-th$ joint's stiffness K_i. Expressions for forces F_1, F_2, and F_3 can be

found from the static analysis of the mechanism or through the principle of virtual work (refer to [10], pp.248-250).

$$F_1 = 3\frac{K_1\Psi_1 cos(\alpha)}{r_2 sin(\vartheta_2 - \alpha)} \tag{7}$$

$$F_2 = 3\frac{K_2\Psi_2 cos(\vartheta_3)}{r_2 sin(\vartheta_3 - \vartheta_2)} \tag{8}$$

$$F_3 = 3\frac{K_3\Psi_3 cos(\vartheta_2)}{l\ sin(\vartheta_2) - e\ cos(\vartheta_2)} \tag{9}$$

where $\alpha = atan(e/l)$ (Fig. 7). Figure 8 shows the moduli of the forces F_1, F_2 and F_3 for the final frame (as calculated via Eqs. 7-9). Let us consider separately the contribution of each stiffness K_1, K_2, K_3: it can be seen that stiffnesses K_1 and K_2 can be chosen such that $F_1 + F_2$ exhibit a quasi-constant FL profile whereas the stiffness K_3 can be chosen such that F_3 exhibit a FL profile with negative slope. In fact, for $K_1 = K_2 = 0$ the compliant slider-crank mechanism becomes a bistable mechanism that reaches an Unstable Equilibrium Position (UEP) when the crank is perpendicular to the slider's direction of motion (i.e. when $\vartheta_2 = \frac{\pi}{2}$). It is well known that mechanisms with this behavior are characterized by FL curves with negative slope (i.e. a force curve with negative stiffness) [7], [8], [10]. As previously discussed in [7], [8] this kind of mechanisms can be designed so as to flatten the DE film FL curve. The design methodology is composed of two steps:

1) The value of K_1 and K_2 are chosen such that:
   - The force sum $F_1 + F_2$ is nearly constant throughout the desired actuator stroke.
   - The force sum $F_1 + F_2$ and the OFF state mode DE film force in the actuator initial position $F_f(\bar{l}, 0)$ and the frame force in the same configuration $F_s(\bar{l})$ have the same moduli.

   Basically a precompressed compliant frame having $K_1 \neq 0$ and $K_2 \neq 0$ is used to offset the actuator available thrust without changing the actuator stiffness.
2) The value of K_3 is chosen so as to flatten $F_f(l, V_{max})$ along the desired range of motion. Note that, in general, the wider the range of motion, the higher will be the deviation of the practically achievable available thrust from the desired constant value.

The characteristic dimensions of the final frame design are found by an optimization procedure widely described in [14], [15] and based on the analytical model presented here. The optimal values for the frame characteristic dimensions are reported in Table II.

In Figure 9, the modulus of the frame force $|F_s|$ (found via PRBM) and the film forces ${F_f}^{on}$, ${F_f}^{off}$ (found by experiments) are plotted as a function of the actuator length l. The frame behavior is as expected: the modulus of the frame force is parallel to the DE film force ${F_f}^{on}$ for a relevant part of the stroke and it coincides to ${F_f}^{off}$ at $l = \bar{l}$.

From the values of K_i, the dimensions of the small length flexural pivots can be derived. Supposing the flexures are straight slender beam hinges with rectangular cross section

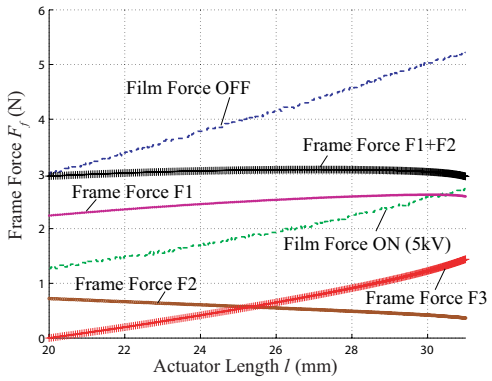

Fig. 8. Frame FL relationship showing the film force F_f (experimental) and the contribution of forces F_1, F_2, F_3 (shown in moduli) on the overall frame force F_s (found via PRBM). Frame dimensions from Table II

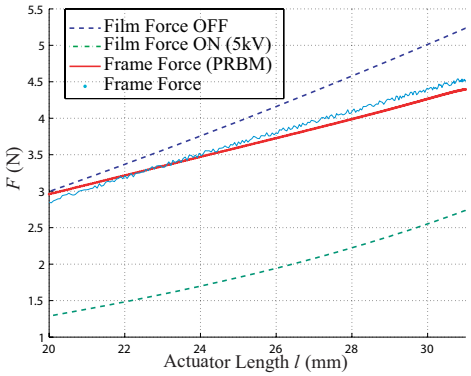

Fig. 9. FL relationship showing film force F_f (experimental) and frame force modulus $|F_s|$ (PRBM and experimental)

then $K_i = EI_{a_i}/L_i$ where E is the frame material Young modulus, L_i is the length of the small-length flexural pivot, and $I_{a_i} = h_i^3 b_i/12$ is the moment of inertia of the pivot cross sectional area with respect to the axis a_i (h_i and b_i denote the pivot thickness and width respectively, whereas a_i is the barycentric axis parallel to the width).

Concerning the frame material, it must be mentioned that the achievement of high strains without overcoming the material yield strength S_y requires a material with a high S_y/E ratio [10]. As is shown in Table III, some plastics, like polypropylene or Teflon (PTFE), offer interesting properties in this respect. However, plastic hinges suffer well-known problems of durability, low fatigue life and time dependent phenomena (like creep or stress relaxation). Therefore, in this paper, metal hinges will be used for the experimental validation of the proposed concept. Nevertheless research is still in progress in order to increase and optimize the achievable fatigue life obtainable with plastic hinges.

Selecting *Sandvik 11R15* as the flexure material and shaping the hinges as simple leaf springs, obtained from steel sheets of the desired thickness, lead to flexure dimensions as reported in Table IV. The frame response has been

TABLE II

COMPLIANT FRAME PARAMETERS

e (mm)	$\bar{l}$ (mm)	r_2 (mm)	r_3 (mm)	r_4 (mm)
28	20	20.9	21.2	12
K_1 (Nm/rad)	K_2 (Nm/rad)	K_3 (Nm/rad)	ϑ_{20} (°)	ϑ_{30} (°)
0.0128	0.006	0.0349	42.0°	221.3°

TABLE III

MATERIAL PROPERTIES IN TERMS OF S_y/E RATIO

Material	E (MPa)	S_y (MPa)	S_y/E x 1000
Teflon (*PTFE*)	345	23	66,7
Polypropylene	1400	34	24,3
Delrin	3100	69	44,9
Steel (*Sandvik 11R15*)	180000	1950	10,5
Aluminum 7075 heat treated	71100	503	7,1

experimentally evaluated (starting from a single leg) using the test set up shown in Fig. 5(b). As depicted in Fig. 9, the experimental results show good agreement with the behavior predicted by the PRBM. Figure 10 shows the overall actuator available thrust F_a. The actuator thrust in the ON state mode is approximately constant (about 1.7N) over the range 20-30mm (in this range a maximal deviation by 0.2 N is admitted) whereas the actuator thrust in the OFF state mode is a linear curve vanishing at an actuator length of 20mm. A positive slope of the available thrust in the OFF state mode shows that the actuator features a returning force which can pull it back when deactivated.

V. CONCLUSIONS

A practical prototype of a Dielectric Elastomer actuator was presented. The actuator is obtained by coupling a conically shaped DE film and a compliant frame. The frame is composed by a fixed base and a moving platform connected by three compliant legs. Each leg behaves as a fully compliant slider-crank mechanism. The proposed frame is used to modify the actuator output so as to obtain a desired profile of the actuator available thrust. The resulting actuator provides a constant force along a relevant part of the stroke when the DE film is activated and a returning force which brings it back to an initial position when the DE film is deactivated. The electromechanical properties of the DE film are measured experimentally whereas the compliant frame was analyzed and sized on the basis of a pseudo-rigid-body model and verified by experiments. Frame and actuator responses are validated via experiments. The proposed actuator works as expected.

TABLE IV

FLEXURE DIMENSIONS

Dimension	b_i (mm)	h_i (mm)	L_i (mm)
Joint K_1	5	0.08	3
Joint K_2	5	0.08	6.4
Joint K_3	5	0.08	1.1

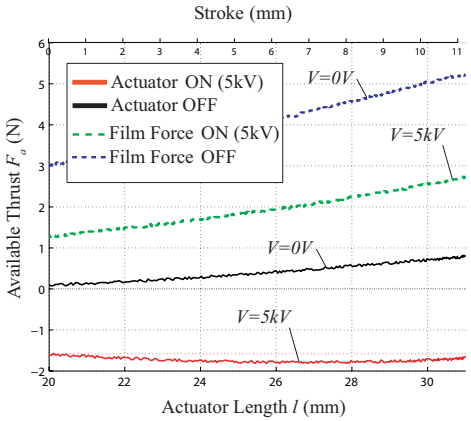

Fig. 10. DE film FL relationship and overall actuator FL relationship

REFERENCES

[1] R.A. Toupin. The elastic dielectrics. *J. Rational Mech. Anal*, 5:849–915, 1956.

[2] J. S. Plante. *Dielectric elastomer actuators for binary robotics and mechatronics*. PhD thesis, Department of Mechanical Engineering, Massachusetts Institute of Technology, Cambridge, MA, 2006.

[3] Helmut F. Schlaak, Markus Jungmann, Marc Matysek, and Peter Lotz. Novel multilayer electrostatic solid state actuators with elastic dielectric (invited paper). volume 5759, pages 121–133. SPIE, 2005.

[4] Y. Bar-Cohen. *Electroactive Polymer (EAP) Actuators as Artificial Muscles: Reality, Potential and Challenges*. Bellingham, WA, SPIE Press, 2001.

[5] L.K. Kim and S. Tadokoro. *Electroactive Polymers for robotic applications*. Springer., 2007.

[6] J. Vogan. Development of Dielectric Elastomer Actuators for MRI Devices. Master's thesis, Department of Mechanical Engineering, Massachusetts Institute of Technology, Cambridge, MA, 2004.

[7] G. Berselli, R. Vertechy, G. Vassura, and V. Parenti Castelli. A compound-structure frame for improving the performance of a dielectric elastomer actuator. *Springer, Advances in Robot Kinematics*, 11:391–398, 2008.

[8] G. Berselli, R. Vertechy, G. Vassura, and V. Parenti Castelli. Design of a single-acting constant-force actuator based on dielectric elastomers. *Proceedings of IDETC/ ASME International Design Engineering Technical Conferences*, 2008.

[9] J.S. Plante and S. Dubowsky. The calibration of a parallel manipulator with binary actuation. *Springer, Advances in Robot Kinematics*, 11:291–299, 2008.

[10] L.L. Howell. *Compliant Mechanisms*. John Wiley and Sons., 2001.

[11] B.D. Jensen and L.L. Howell. Bistable configurations of compliant mechanisms modeled using four links and translational joints. *ASME Journal of Mechanical Design*, 126:657–666, 2004.

[12] C. Bolzmacher, M. Hafez, M. B. Khoudja, P. Bernardoni, and S. Dubowsky. Polymer based actuators for virtual reality devices and rehabilitation applications. In *Proceedings of the SPIE*, volume 5385, pages 281–289, 2004.

[13] Huaming Wang and Jianying Zhu. Implementation and simulation of a cone dielectric elastomer actuator. volume 7266, page 726607. SPIE, 2008.

[14] L. L. Howell, A. Midha, and M. D. Murphy. Dimensional synthesis of compliant constant force slider mechanisms. In *Proceedings of DETC94, ASME Design Engineering Technical Conferences*, volume 71, 1994.

[15] B. L. Weight. Development and design of constant-force mechanisms. Master's thesis, Department of Mechanical Engineering Brigham Young University, 2001.